Accepted Manuscript

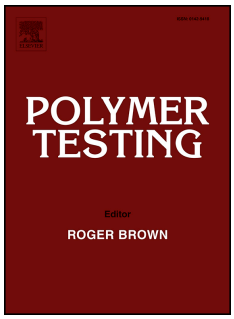

Study of an alternative material to manufacture layered hydraulic hoses

Geovana Drumond, Ilson Pasqualino, Marysilvia da Costa

PII: S0142-9418(16)30020-4

DOI: 10.1016/j.polymertesting.2016.05.003

Reference: POTE 4648

To appear in: *Polymer Testing*

Received Date: 8 January 2016

Revised Date: 11 April 2016

Accepted Date: 4 May 2016

Please cite this article as: G. Drumond, I. Pasqualino, M. da Costa, Study of an alternative material to manufacture layered hydraulic hoses, *Polymer Testing* (2016), doi: 10.1016/j.polymertesting.2016.05.003.

Study of an Alternative Material to Manufacture Layered Hydraulic Hoses

Geovana Drumond[1], Ilson Pasqualino[2], Marysilvia da Costa[3]

[1,2]Departmentof Ocean Engineering, Federal University of Rio de Janeiro, Brazil

[3]Department of Metallurgical and Materials Engineering, Federal University of Rio de Janeiro, Brazil

ABSTRACT

Hydraulic hoses are components of umbilical cables and others subsea equipments. They are manufactured from thermoplastic polymers and are susceptible to collapse under external pressure, which can cause plastic strains around the circumference, leading to failure under internal pressure (bursting). This work studies an alternative hydraulic hose liner capable of support such load history, even after long time exposure to the hydraulic fluid. It is based on the comparison between the material currently used (Polyamide 11) and a fluorinated elastomer, Viton®. Mechanical characterization, ageing tests as well as nonlinear finite elements simulations were accomplished to issue both performances. The results obtained showed that Viton® liners are mechanically more suitable than Polyamide 11 liners to such hoses. The ageing tests showed compatibility between Viton® and the hydraulic fluid. Considering that the external aramid layer is responsible to withstand the internal pressure in both cases, Viton® can successfully replace Polyamide 11 for this application as well as others involving layered hoses under combined internal and external pressure.

Keywords: Hydraulic Hoses, Numerical Simulations, Pressure Loads, Ageing in Hydraulic Fluid, Mechanical and Thermal Analysis

1. INTRODUCTION

In recent years, offshore oil and gas exploration has rapidly advanced to record water depths that were beyond conception 20 years ago, and in this scenario of deep and ultra deep-water, layered hose structures assume an important role. Among them, umbilical control cables are of major importance. These cables are designed to deal with harsh environments, changes in temperature, sea currents, waves, winds and platform offset. During production, such equipment is responsible for controlling xmas tree block valves, down hole safety valves and subsea control modules (SCMs) in manifolds. In general, subsea umbilicals comprise an assemblage of HCR (High Collapse Resistance) hoses for chemical injection, thermoplastic hoses to hydraulic control of valves, electrical cables, tensile armors and polymer inner and outer layers.

Hydraulic hoses specifically may have three or four layers depending on the operational conditions. The inner layer is typically made of Polyamide 11 (PA11). The annular layers, one or two depending on the pressure to be supported, are made of aramid fiber (Kevlar®) and the outer layer is made of Polyurethane or PU (Figure 1). A typical umbilical cable may have several of these hoses.

Author for correspondence: Geovana P. Drumond, Subsea Technology Laboratory, COPPE/UFRJ, ZIP code: 21941-450, Rio de Janeiro, RJ, Brazil. E-mail: geovana@lts.coppe.ufrj.br

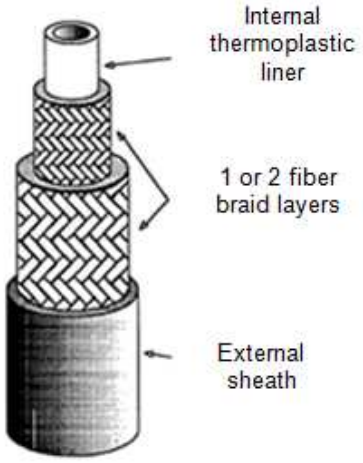

Figure 1: Typical Umbilical Hose Structure [1]

Failures in umbilical cables have been reported in recent works. Rabelo [2] has studied several installations and inspection reports, publications of operators and manufactures appointments in order to record the major non-compliances that have occurred with subsea umbilical cables. The research correlated failures in thermoplastic hoses with aspects concerning their conception and pointing at the hose limited resistance to collapse as the likely reason for the failures described. Due to the limitation mapped, it was established as a premise of umbilical design that hoses should be kept filled with pressurized working fluid during all the installation procedure, regardless of the water depth. The collapse is presented as a phenomenon caused by the gradual rise of a compressive load, shortening the structure to its limit and reducing its compression stiffness up to instability. In the case of hoses, which behave as cylindrical shells, the external pressure application generates instability, manifested through the gradual increase of ovalization induced by initial imperfections.

Although the umbilical failure is largely associated to the hose, the most common method adopted to assess the umbilical's suitability has been to employ models of the umbilical whole structure (when available) using empirical and mathematical techniques based upon historical data and which are validated through expensive full-scale testing. Due to the diversity of design of umbilical structures, it is necessary to employ a high degree of conservatism in the design analysis to ensure sufficient confidence in the analysis outcome [3]. A 3D umbilical simulation tool, known as 3DUST [4] is capable of three-dimensional modeling and consists of pre-processing and post-processing features. This kind of tool is widely used nowadays for global analysis, like the calculus of installation capacity such as bending, axial load, crush load and ovality of the umbilical. Few authors used 3D numerical simulations to study the behavior of umbilical cables with good results like Pesce et al. [5], Dixon and Zhao [6] and Le Corre and Probyn [7]. None of them focused on the behavior of the hydraulic hoses and its layers though.

It was not found any model dedicated to evaluation of the layered hoses and its mechanical behavior when subjected to cyclic stresses. Studies on the hose itself are usually related to the evaluation of material

chemical stability when in contact with the transported fluids. These studies are either concerned with ageing of the thermoplastic and how the different fluids will affect its lifetime [8], [9], [10], with fluid permeation [1] or with the effect of the material response to rapid pressure changes [11]. Several of these works propose the use of different materials to overcome problems associated to chemical stability, usually thermoplastic polymers with improved properties such as crosslinked polyethylene [1]. Although such studies are indeed crucial for materials evaluation, they are not sufficient once failure may not be associated to the materials ageing, but rather to a lack of mechanical endurance.

The present work analyses the collapse of a layered hose structure since it has been established as one of the most important source of failure for umbilical cables [2] and no similar study was found in literature. Based on the behavior observed, the authors propose that PA 11 could be replaced by a hyperelastic material, namely a fluoroelastomer, which would avoid the main cause of hose failure since it would be less subject to plastic deformation. Therefore, a theoretical study and an experimental analysis of material compatibility were carried. The theoretical study was based on a nonlinear finite element model developed with the aid of ABAQUS software. The aim was to study the behavior of a conventional hydraulic hose under combined loading of internal and external pressure, considering different materials for liner layer. This same model can be applied to several types of layered hose in subsea or other applications. To propose the replacement of PA 11 by an elastomeric liner, it is essential to prove that the fluoroelastomer does not interact with the hydraulic fluid, and for that, a preliminary chemical compatibility test was carried out, with a water based fluid, to verify if the polymer does not lose mass or undergo swelling, and also if the mechanical properties are preserved.

2. MODEL

The model comprises the two dimensions cross-section of a three layers structure representing the hydraulic hose, as shown in Figure 2. Both, inner and outer layers, were discretized using continuous solid elements of the type CPE4H, detailed in the ABAQUS Elements Manual [12]. The CPE4H defines a first order quadrilateral element with four nodes and two translational degrees of freedom per node and uses a bilinear interpolation and hybrid formulation to deal with incompressible material behavior. For the intermediate Kevlar® layer, truss elements of the type T2D2 were used. This element has two nodes with two translational degrees of freedom per node and uses linear interpolation to calculate displacements. In order to simulate cable elements compression rigidity was disabled. According to mean radius and thickness (0.88 mm) values, a cross sectional area equals to 0.774 mm^2 was defined for the cable layer. The geometry was obtained from laboratory measurements on hose samples provided by industry and dimensions for each layer are shown in Table 1. The model was simplified to minimize computational processing time assuming half section symmetry (Figure 2).

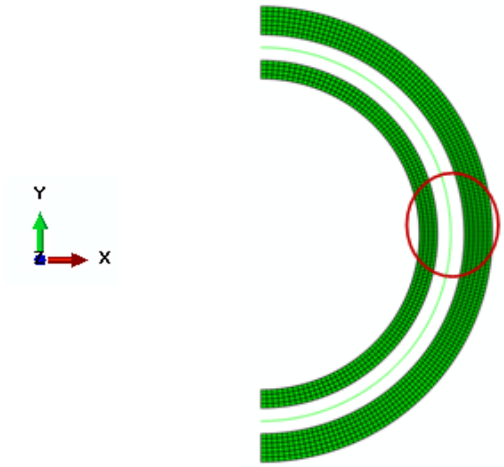

Figure 2: Mesh of the Three Hydraulic Hose Layers

Table 1: Geometric Parameters of Layers

Layer	Inner Radius (mm)	Outer Radius (mm)	Thickness (mm)
Inner (PA 11)	5.225	5.825	0.60
Intermediate (Kevlar®)	5.825	6.705	0.88
Outer (Polyurethane)	6.705	7.635	0.93

Hydraulic hoses have imperfect geometry (initial ovalization). This occurs due to manufacture processing, handling and installation. To simulate such imperfection, Equation 1 with initial ovalization (Δ_0) of 1% was used.

$$w_0 = R.\Delta_0.cos\,2\theta \quad (1)$$

where *R* is the outer radius and θ varies from y = 0° to y = 90° or to -90°.

For model meshing, the region of interest, highlighted in red in Figure 2, is where the larger strains will be localized. This region was better refined in relation to the other areas of the hose section. The mesh refinement was controlled by element size (0.1 mm long at region of interest), making this region twice more refined than the others (0.2 mm long). This refinement is used for the three layers. The inner layer was represented with four elements in thickness while six elements were used to the outer layer (Figure 2).

Different constitutive models assuming large rotations and large strains were used to characterize the behavior of each material under external and internal pressure loads. For the aramid layer, the finite element model was defined assuming a linear elastic isotropic behavior. The manufacturer of Kevlar29® provided the values of 70500 MPa and 0.36 for Young's modulus and Poisson's coefficient, respectively. Such values are fiber's properties but do not represent woven properties. For transversal section simulation, the hoop direction

properties are needed. Figure 3 illustrates the Kevlar® braid geometry, where it can be observed the components of Young's modulus.

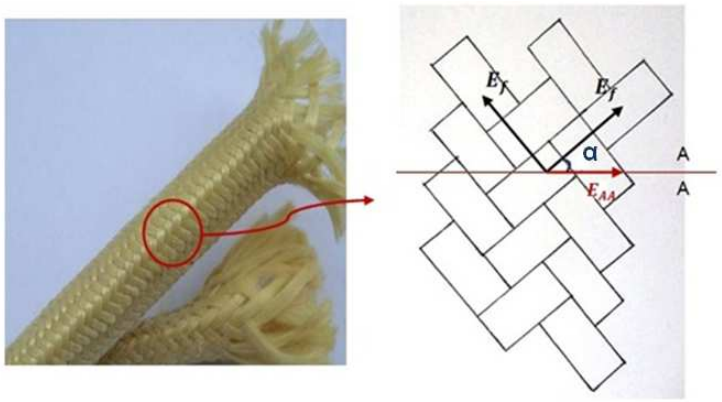

Figure 3: Calculus of the Young's Modulus of Kevlar® Braid

In Figure 3, the elasticity modulus in cut AA plane is defined by the following equation:

$$E_{AA} = E_f \cos \alpha \tag{2}$$

where E_f is the Young's modulus in fiber direction; α is the angle between the fiber direction and cut AA; and E_{AA} is the Young's modulus in cut AA plane. Using hose samples given by industry, α was measured as 12°. From E_f (70500 MPa), the Young's modulus equal to 68960 MPa was calculated.

PA 11 was modeled assuming elastic-plastic behavior, no viscoelasticity and a potential flow rule within the von Mises yield criterion under isotropic or combined isotropic and kinematic hardening. The values of Young's modulus and Poisson's coefficients used are 300 MPa and 0.31, respectively obtained for tensile curves as described in the experimental section. The Bauschinger effect was included in the model assuming combined hardening capability in the analysis in order to represent possible effects of drawing of the PA11 due to extrusion. Even though the specimens employed in the experimental data were not extruded, therefore not subject to a previous orientation, anisotropy is considered in the model.

Viton® and Polyurethane layers were modeled assuming hyperelastic behavior following the Yeoh method, where strain energy function can be applied to deduce the stress-strain relations and tangent stiff matrix during deformation [13]. These strain energy functions are set by a number of coefficients called the hyperelastic parameters. Using the Yeoh method, ABAQUS internally calculates the value of those coefficients and adjusts the mean stress-strain curve given as input to the model.

The contact between different layers was defined through ABAQUS contact surfaces, in which internal elements are generated to simulate the contact pairs. In addition, the contact between the internal hose surface was defined to properly represent the hose collapse.

Normal displacements are restricted at x=0 (global Cartesian system) to simulate the symmetry condition. Displacements in y direction are constrained at $y=0$ to avoid rigid body motion. The external pressure is applied to the external surface of Polyurethane layer while internal pressure is applied in the internal surface of PA 11 or Viton® layer. A nodal cylindrical coordinate system was used for load application and results post processing. In this way, the planar components to be mentioned are in radial and hoop directions.

3. MATERIAL AND METHODS

PA11 dog bone specimens, Type I, were obtained by compression molding of PA 11, umbilical hose grade, under a load of 6 tons for five minutes at 220°C followed by a controlled cooling carried out at 80℃ under a load of half a tonne for ten minutes. After this time, another cooling was performed, now at room temperature, for five minutes. Conditioning of PA 11 was made with 50% of humidity. The specimens are standardized according to ASTM D 638 [14] (Type I).

Viton® was obtained from Dupont, and PU of 85 Shore A hardness and MOCA crosslinking agent was obtained from Plastiprene. Tensile specimens according to ASTM D 412 [15] with a 25 mm of gage length were cut from 3 mm thick blankets for Viton® and machined from 10 mm thick blankets for PU. For Viton®, cylindrical shape samples with a diameter of 13 mm and height of 6.5 mm (ISO 7743 [16]) were cut for compression and hardness tests.

Tensile tests for PA 11 were carried according with ASTM D 638 [14], in an INSTRON universal testing machine equipped with a 10kN load cell. Tests were carried at a crosshead speed of 50 mm/min at room temperature. The strains were measured with the aid of an advanced video extensometer (AVE) system. For Viton®, non-aged and aged, and PU the same equipment was employed but tests were carried according with ASTM D 412 [15] at a crosshead speed of 500 mm/min at room temperature.

The interaction between Viton® and the hydraulic fluid was evaluated through compatibility test. Sets of standardized test samples were immersed in a hydraulic fluid (HW-525, with 20 to 25% of glycol, 1 to 5% of lubricants and 75% of distilled and deionized water) at a temperature of 60℃ for a period of 270 days. Mechanical tests (tension, compression and hardness) and thermal analysis (DMA, DSC and TGA) were carried out to five ageing times: 15, 30, 60, 120 and 270 days. In addition, after each removal, samples were dried and weighed for mass variation control. After each weighing, the samples were returned to the bath for ongoing tests.

For hardness test (ASTM D 2240 [17]), an INSTRON 9130-035 durometer with 1kgf load was used. According to the standard, the indenter must be pressed on the sample during 10 seconds in five random points.

Compression tests (ISO 7743 [16]) were also carried out in the same Instron universal testing machine at room temperature and a crosshead speed of 10 mm/min. The metal plates were lubricated to minimize friction. The deformation was taken by the machine crosshead displacement and tests were carried up to a strain of 25%. The strain was then released at the same crosshead speed of 10 mm/min to a new cycle of compression, up to the accomplishment of three cycles according to the standard procedure.

A DMA 242 NETZSCH was used to measure the mechanical relaxation of the polymer samples. The analysis was done by compression of the samples with dimensions of 12.5 mm in diameter and 5 mm in thickness. The tests were done in accordance with ASTM E2254 [18]. Dynamic and static forces of 6 and 0.4 N, respectively, were kept constant from -50 to 100℃. The heating rate was 2 ^{o}K/min under a nitrogen atmosphere (50 ml/min). The testing frequency was 1Hz to an amplitude of 30 µm.

A PerkinElmer PYRIS 1 TGA was used to determine mass loss of polymer samples as a function of increasing temperature. Thermogravimetric analysis was based on ASTM D6370 [19]. Samples weighing between 7 and 10 mg were heated from 20 to 500℃ in an inert atmosphere (nitrogen) at a rate of 20 ℃/ min. After that, the oven atmosphere was replaced by oxygen until the temperature of 800℃.

4. RESULTS

4.1. Numerical Model Results

Figure 4 shows a typical tensile curve obtained for Viton® (a), PU (b) and PA 11 (c). The stress-strain properties derived from the tests were used as input data for the numerical models.

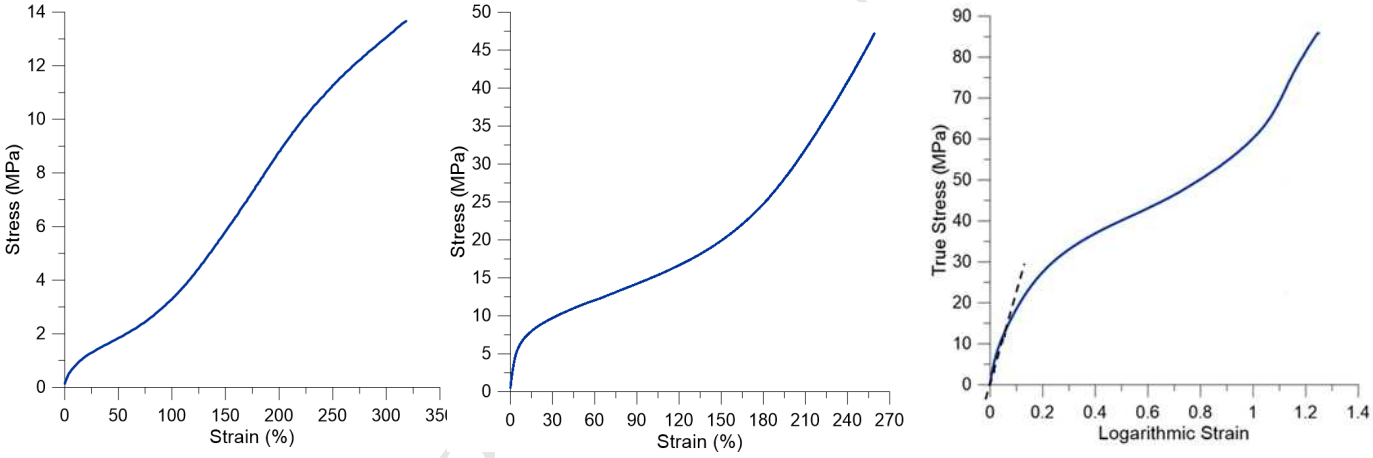

(a) (b) (c)

Figure 4: Stress versus Strain Behavior for (a) Viton®; (b) Polyurethane and (c) PA 11

The theoretical results were obtained from the nonlinear FE model described above. They are discussed from the interpretation of the surfaces of the von Mises equivalent stress, equivalent plastic deformation (PEEQ) and hoop component of logarithmic deformation (LE22).

A first analysis was carried to determine the liner behavior of a conventional hydraulic hose, made in PA 11, under a collapsing external pressure followed by an internal pressure generated by the surface pressure unit. For the first step, an external pressure as low as 2 MPa was enough to collapse the section without model divergence.

Under external pressure, the hose experienced high von Mises stresses, up to 48 MPa, and an equivalent plastic deformations of around +48%, as can be seen in Figure 5. For hoop strain components, a total deformation (elastic+ plastic) of around -58% was observed.

Under an internal pressure of 15 MPa, the PA 11 liner and the Kevlar® layer presented von Mises equivalent stresses up to 55 MPa and 110 MPa (Figure 6(a)), respectively, since the later undergo high elastic stress to resist internal pressure. On the other hand, the equivalent plastic deformations of PA11 were further increased to +76% at the localized plastic hinge (Figure 6(b)). The liner also presented +4.7% to -1.9% of total hoop logarithmic strains at the plastic hinge in view of the sum of residual strains and the ones generated by the internal pressure (Figure 6(c)).

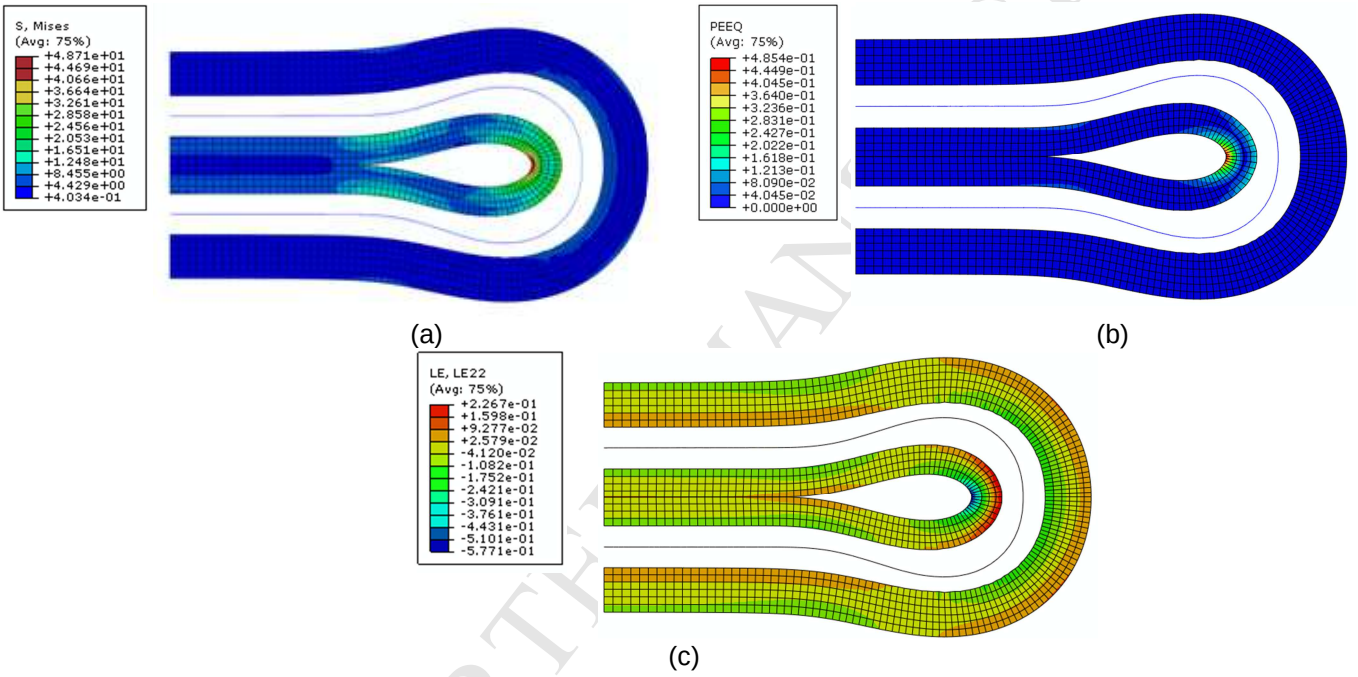

Figure 5: (a) Stress; (b) Equivalent Plastic Strain (PEEQ); (c) Total Logarithmic Strain under External Pressure of 2 MPa

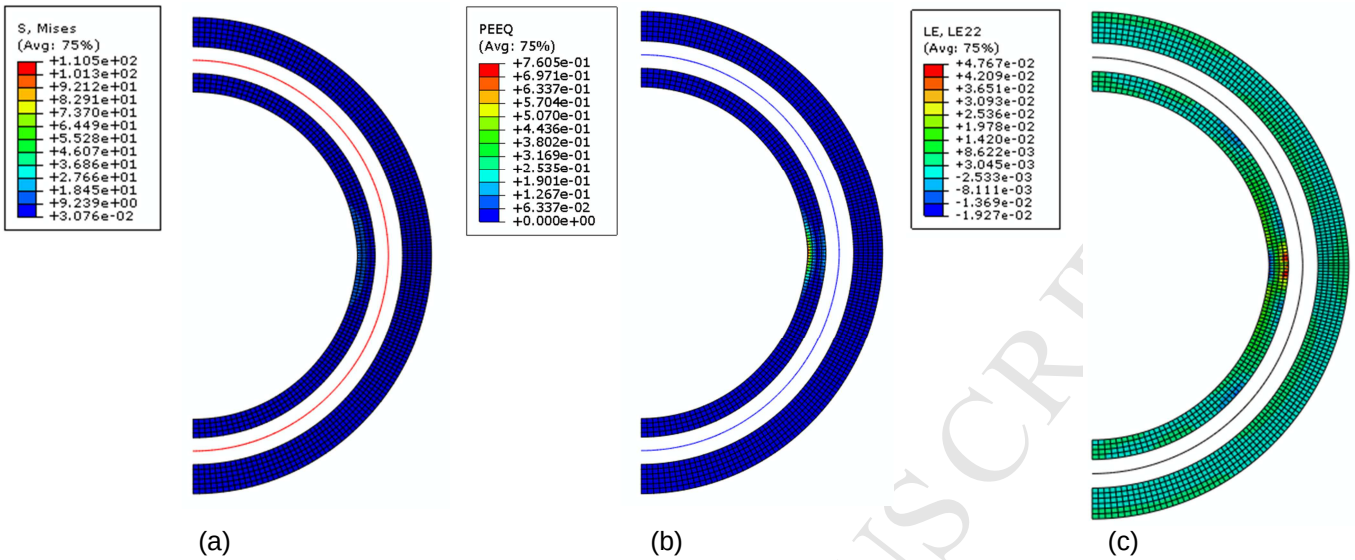

(a) (b) (c)

Figure 6: (a) Stress; (b) Equivalent Plastic Strain; (c) Total Logarithmic Strain under Internal Pressure of 15 MPa

In a second study, the elastic-plastic PA 11 layer was replaced by the hyperelastic Viton® material. The same geometry, boundary conditions and loads were used but the FE mesh refinement was adapted to obtain a good balance between results accuracy and CPU time.

When the external pressure was applied, the hydraulic hose comprised of the “soft” Viton® liner fully collapsed. Therefore, the total hoop strain went up to 66% (Figure 7(b)) at a low level of equivalent stress, not greater than 18 MPa (Figure 7(a)). In spite of the high strains exhibited, no plastic deformation has occurred since it is not foreseen by the constitutive model or experimental response of a hyperelastic material as Viton®.

Different from the PA 11 liner under internal pressure, Viton® did not concentrate stress or strain after collapsing, as can be observed in Figure 8 (a) and (b), respectively. The von Mises stress was low, 9 MPa, while the Kevlar® layer withstood all internal pressure, being stressed up to 110 MPa. In addition, the maximum hoop strain was less than 19%.

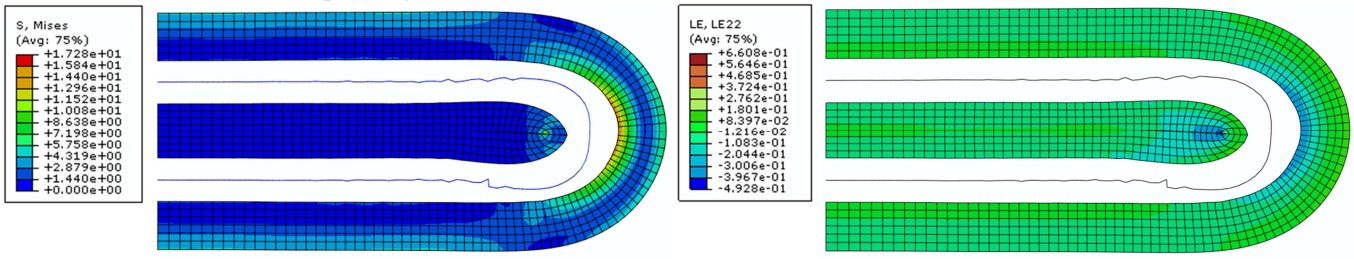

(a) (b)

Figure 7: (a) Stress; (b) Total Logarithmic Strain under External Pressure of 2 MPa

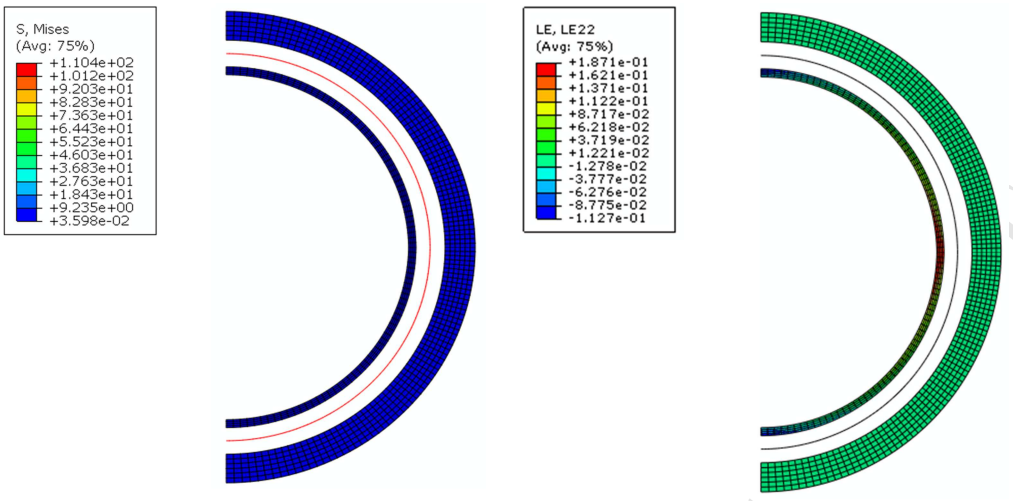

(a) (b)

Figure 8: (a) Stress; (b) Total Logarithmic Strain under Pressure of 15 MPa

The results obtained by the numerical analyses are summarized in Table 2, and it is clearly observed that stress and even strains are smaller when Viton® liners are employed. The remarkable feature about Viton® is not to accumulate permanent strains, different from PA 11 where permanent strain levels increase from the first to the second load step. It is also possible that some type of ratcheting (progressive strains) may occur within PA 11 layer in an actual situation of cyclic internal/external pressure since such phenomenon has been reported to other thermoplastic materials under uniaxial and multi axial loading [20], [21], [22] and this could be a reason for the failures reported in those PA 11 hoses.

The low-stress level at Viton® layer is explained by the Kevlar® braid that is highly stressed and withstands the internal pressure. Therefore, the same low stresses should have been observed for PA 11 if plastic hinge was not generated under the external pressure. It can be seen in Figure 6 that stress and strains are low at the regions outside the plastic hinge. Then internal pressure is not high enough to burst the hose because the Kevlar® braid supports it and, unless some extrusion of the material into the fibers occurs, the liner does not need to be rigid but only elastic enough to avoid plastic strains. Therefore, it is possible that the thermoplastic liner could be replaced by a hyperelastic one if only structural requirements are considered. There are not other studies in literature proposing such a drastic modification in terms of umbilical composition. A prior study [1] proposes replacement of PA 11 by other thermoplastic, but according with the results shown in this work, this solution may not be effective since thermoplastic polymers will always be subject to plastic deformation that will be even aggravated if ratcheting occurs.

Table 2: Extreme Strain and Stress Values for PA 11 and Viton® Liners

Liner Material	External Pressure (2 MPa)			Internal Pressure (15 MPa)		
	Von Mises Stress (MPa)	Equivalent Plastic Strain	Total Logarithmic Hoop strain	Von Mises Stress (MPa)	Equivalent Plastic Strain	Total Logarithmic Hoop strain
PA 11	48	0.48	-0.58	55	0.76	+0.047
Viton®	10	---	-0.49	9	---	+0.18

A phenomenon often found in oriented polymers is a pronounced asymmetry between the tensile and compressive responses that is not present in isotropic polymers. A classic example of such a response in hydrostatically extruded polypropylene was presented by Mohanraj et al. [23], who measured a tensile yield stress that was about 8 times higher than the compressive one for an extrusion ratio of 5. PA 11 presents such asymmetry and this phenomenon is expected to be even more drastic for processing that induces drawing, as is the case of extrusion, the technique used for hose fabrication. This type of asymmetry is often referred as the Bauschinger effect, named after a phenomenon in metals that has quite similar phenomenology, but a different physical background. According to Senden et al. [24], for semi-crystalline polymers, the influence of processing induced orientation is particularly large due to the material microstructure, which is a heterogeneous composition of intrinsically anisotropic crystalline domains and randomly coiled amorphous regions. There was not found in literature any work about processing induced orientation in elastomers and so, those effects were not considered for Viton® and Polyurethane. Therefore, a third study was carried to include the effect of this induced orientation.

In order to evaluate the behavior of PA 11 when submitted to higher levels of pressure, a hose at approximately 500 m of water depth and 5000 psi of working pressure experiencing load levels of about 5 MPa was considered. Using the same mesh of the previous model, 5 MPa of external pressure was applied followed by 35 MPa of internal pressure. Aiming to know if the Bauschinger effect (combined isotropic and kinematic hardening) changes the deformation field experienced by the hose, two different constitutive models, considering isotropic hardening or combined isotropic and kinematic hardening plasticity, were applied to the PA 11 layer.

Figure 9 compares the collapsed section of the PA 11 under 5 MPa of external pressure without (left) and with (right) the Bauschinger effect. It can be verified that the Bauschinger effect assumption increases the maximum plastic strain from 67 to 74% approximately and makes the strain field less concentrated than the isotropic hardening model. In addition, there was a significant increase of the maximum plastic strain relative to the value in the first model (48%), when it was considered an external pressure of 2 MPa.

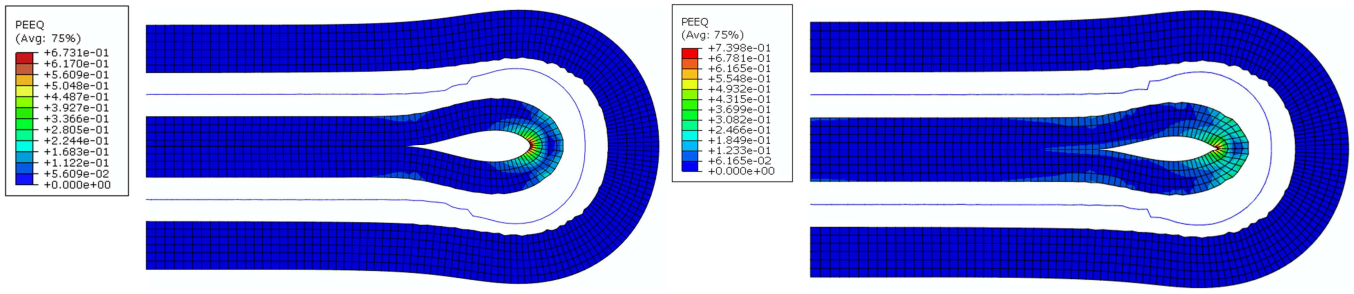

(a) (b)

Figure 9: Equivalent Plastic Strain (a) without and (b) with Bauschinger Effect under External Pressure of 5 MPa

The uncollapsed section under internal pressure of 35 MPa is presented in Figure 10. Again, the Bauschinger effect model resulted in higher plastic strains (138%), which are very close to materials limit, reported as 140% from the uniaxial tension test (Figure 4(c)). Even if material behaves under the isotropic hardening model, the maximum plastic strain achieved is still high.

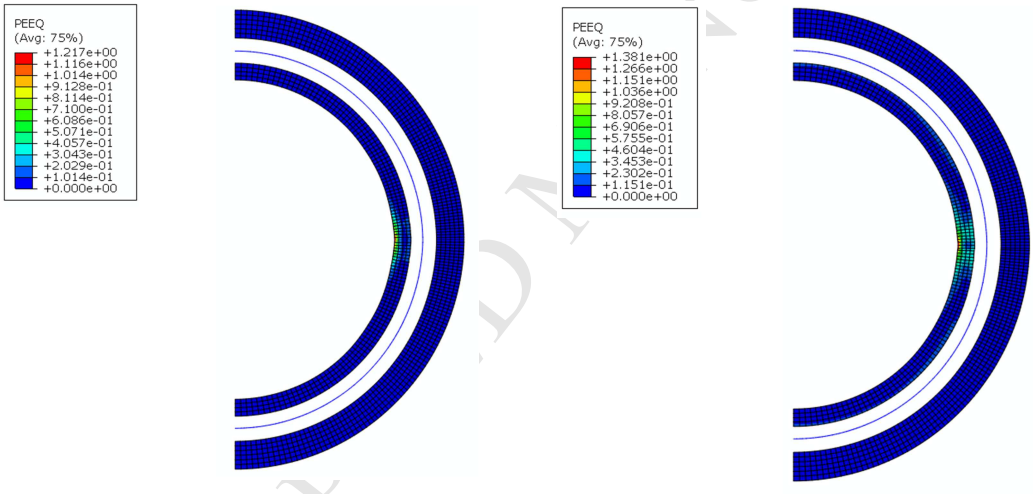

(a) (b)

Figure 10: Equivalent Plastic Strain (a) without and (b) with Bauschinger Effect under Internal Pressure of 35 MPa

Besides the comparative study (PA 11 versus Viton®), it was investigated from a numerical approach if operational loads (5 and 35 MPa of external and internal pressure, respectively) were capable of failing a PA 11 liner of a hydraulic hose. To study possible changes in PA 11 response due to the inclusion of Bauschinger effect, two simulations were made: considering isotropic hardening and combined isotropic and kinematic hardening plasticity model for PA 11 layer. The results are summarized in Table 3.

Table 3: Extreme Strain and Stress Values for Different Plasticity Models of PA 11

Constitutive Model	External Pressure (5 MPa)			Internal Pressure (35 MPa)		
	Von Mises Stress (MPa)	Equivalent Plastic Strain	Total Logarithmic Hoop Strain	Von Mises Stress (MPa)	Equivalent Plastic Strain	Total Logarithmic Hoop Strain
Isotropic Hardening	51	+0.67	-0.77	70	+1.21	0.10
Combined Isotropic and Kinematic Hardening	63	+0.73	-0.79	34	+1.38	0.08

The results related to both constitutive models show extremely high strains under the operational loads to a PA 11 liner. If other sophisticated mechanical effects, like ratcheting, low cycle fatigue or even the viscous behavior have been modeled, the simulations could reproduce the failures reported under field operation. Here, only high plastic strains were obtained, but the actual failure mode to justify the liner rupture is the subject of further studies. Unfortunately, these models require many mechanical properties obtained experimentally and this is not the aim of this work. In case Bauschinger effect is considered, the obtained von Mises stresses are smaller but the equivalent plastic strains are higher. This can be preponderant to achieve the maximum tensile strain after only one cycle of collapse followed by internal pressure.

4.2. Compatibility Test Results

Compatibility tests were carried out in order to perform a preliminary evaluation if the Viton® proposed to replace PA 11 was chemically resistant to the hydraulic fluid as well as to determine if any possible changes on tensile and compression behavior due to fluid absorption could prevent the material to be employed for this specific application. Figure 11 shows the behavior of mass variation with time for the Viton® immersed in a water based hydraulic fluid. It is observed that, after 270 days of immersion, mass variation was below 5%. Moreover, the absorption mechanism seems to change between 120 and 270 days. Up to 120 days, the absorption is linear with $t^{1/2}$ and a sudden increase in fluid uptake is observed after that, indicating a change on the kinetics of the absorption process at the evaluated conditions. Physical and mechanical characterization was then performed comparing the aged and non-aged material to consider if the changes that took place due to the fluid are important on the performance of the material.

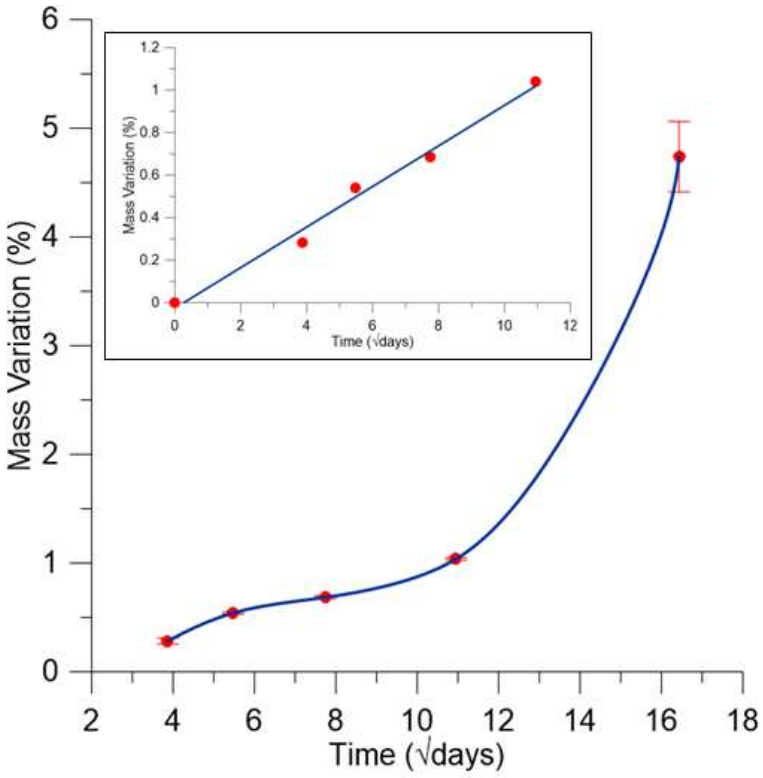

Figure 11: Mass Variation during Compatibility Test

Thermal stability of the fluoroelastomer was evaluated by TGA. Figure 12 shows the percentage variation of the weight loss and the derivative of the percentage weight loss with temperature for non-aged material and after 270 days of immersion. Three steps can be identified for both conditions. In the first step, between 0℃ to 450℃, the weight loss was about 1% for the non-age d material and 8.45% for 270 days of immersion. This first step corresponds to the loss of volatile components. The second step comprises the pyrolysis (thermal degradation) of the elastomer itself, and took place between 450 and 600^{o}C. For this step a mass loss of around 79% for non-aged material, and 68% for the 270 days aged material was observed. The residue formed in the third step was about 9% for non-aged material, and 24% for 270 days aged material. It can also be noted, by DTG curves, that the main mass loss event shifted about 10^{o}C to lower temperatures with the immersion time, dropping from 535^{o}C to 524^{o}C, with a rate increase from -44.3%/min to -76.7%/min.

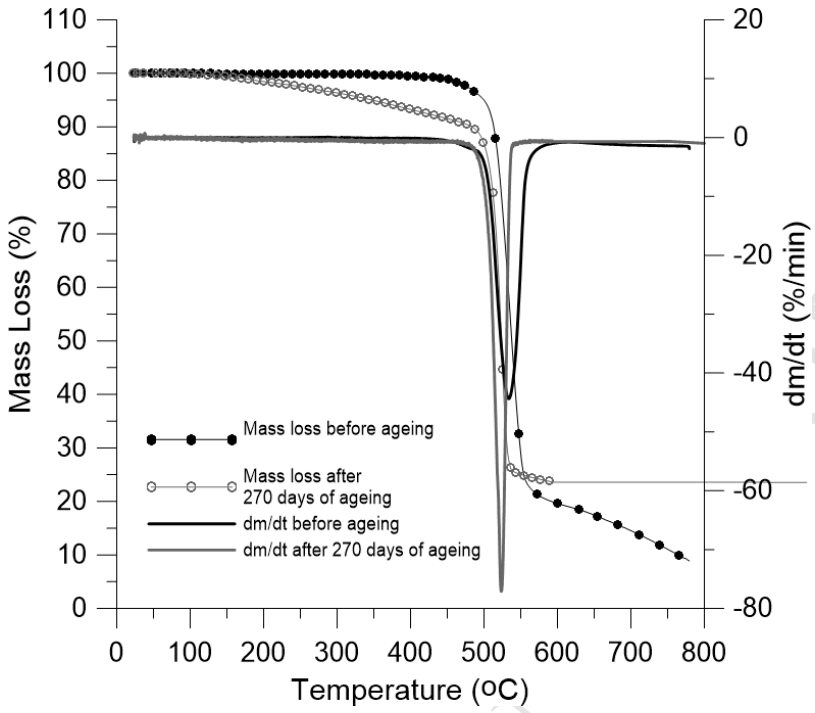

Figure 12: TGA and DTG Curves for Aged and Non-Aged Samples of Viton®

TGAs results clearly indicate that this particular fluid affects the thermal stability of the material. Thermal decomposition of fluoropolymers, in general, is very complex [25]. For fluoroelastomers in particular, the degradation mechanism will depend on the overall composition, including monomer, cure agent and additives [26]. In a very simplified interpretation, two competing decomposition processes are expected: decomposition by scission of the carbon bonds of the backbone chain, and decomposition by scission of adjacent pendent hydrogen and fluoride with formation of hydrogen fluoride. If the first mechanism is predominant, no residues is expected to be formed once the process will advance with random initiation that will lead to formation of macroradicals that, in turn, will propagate and then terminate through the more favorable mechanism (disproportionation and/or combination). On the other hand, if the second mechanism is predominant, residue will be generated. Crosslinking can also be formed or split off during thermal decomposition and the mechanism is also susceptible to be modified due to the presence of the fluid.

The increase on the percentage of weight loss in the first step observed in Figure 12 can be attributed to volatilization of the fluid absorbed and/or to an increase in the amount of small molecules that could be formed during the immersion period. It is interesting to note also that, besides decreasing the T_{max} in 10°C, the main decomposition process is faster and occurs in a narrower temperature window, with formation of a larger amount of residues. This strongly indicates that the thermal decomposition mechanism after immersion is affected and therefore, fluid and material interacts. Moreover, the increase in the residue observed indicates that the predominant degradation mechanism is not breaking of the backbone chain.

Shore A surface hardness measurements were not very decisive on elucidating how fluid is affecting the

fluoroelastomer. Taking the time of 10 seconds of indentation indicated by ASTM D2240 [17] as a reference, a tendency on hardness decrease is observed though, as shown in Figure 13, that would be indicative of break of the crosslink bonds. The results are scattered for the initial 90 days of immersion and tend to stabilize after 120 days (reduction of just 0.6%, from 65.2 after 120 days to 64.8 after 270 days of ageing). This oscillation is consistent with the complex mechanisms involved as mentioned above.

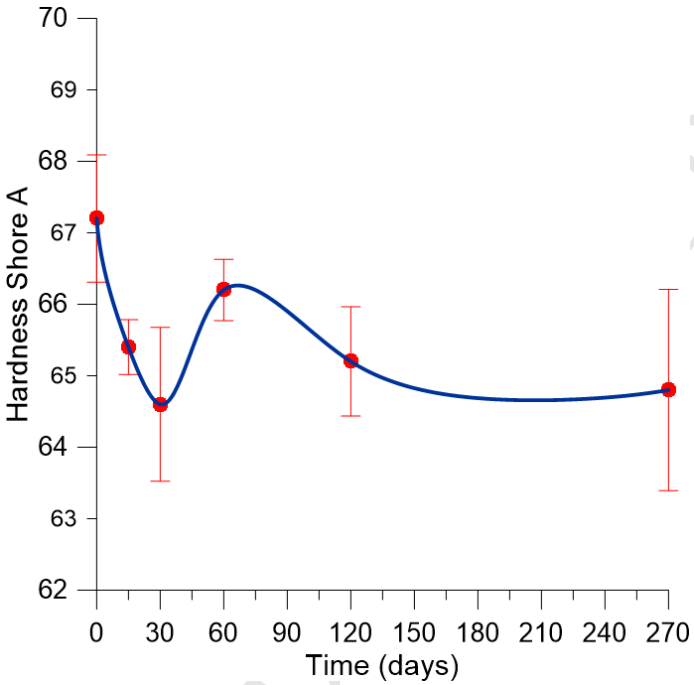

Figure 13: Hardness Shore A with 10s of Indentation versus Time of Ageing

This decrease in rigidity can also be identified in the DMA analysis. Figure 14 shows the *tanδ* curves for the different immersion times compared to the non-aged sample. Clearly, after immersion, the peaks shift to lower temperatures become broader, indicating that molecular motion is facilitated over a wider range of temperature. This offset is probably due to the absorption and interaction of hydraulic fluid with Viton®, which promoted mobility of polymer chains, making the glass transition occurs at smaller temperatures. Analyzing the curves of *tanδ* we notice a reduction of 3.6^{o}C in *Tg* values for the first 15 days of ageing (from 10.3 to 6.7^{o}C). Between 15 and 60 days, the values remain around 7^{o}C. After 120 days of ageing, the *Tg* value has a reduction of 4.3^{o}C in comparison to the beginning of the test (from 10.3 to 6^{O}C). However, at the end of the test, it can be observed an increase in *Tg* value, from 6^{o}C (120 days) to 8.5^{o}C (270 days), showing a clearly change in the degradation mechanism of the fluoroelastomer. These values are shown in Table 4.

This is even more significant because the experiments were carried under compression load where free volume effects tend to be minimized and the system loose mobility. Although the maximum peak value does not show a systematic increase, no additional relaxations with aging time are perceptible.

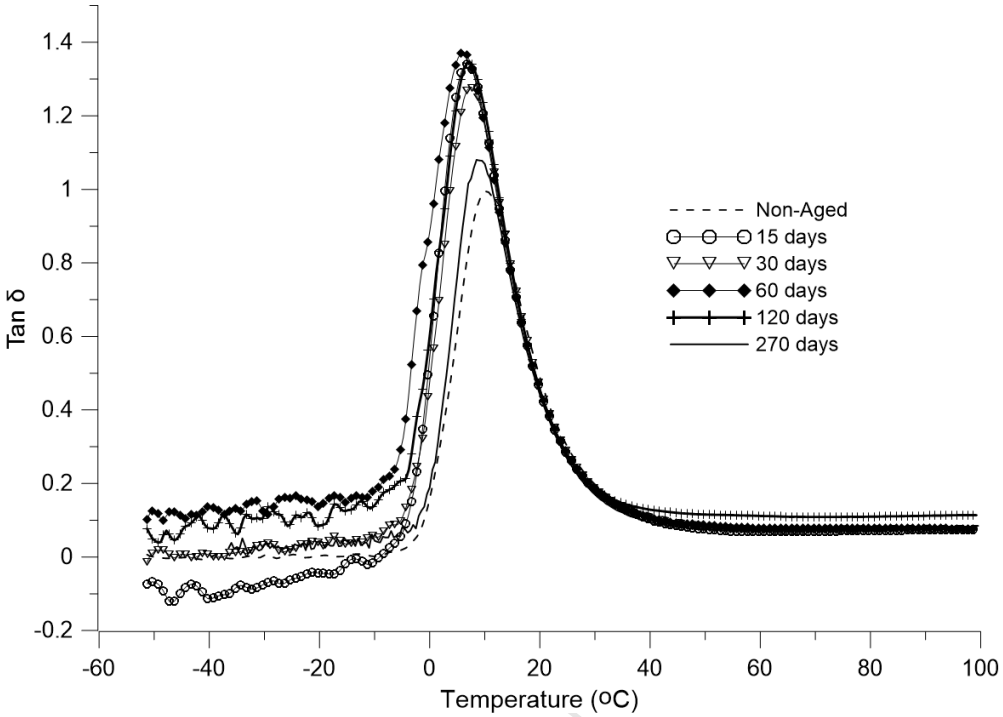

Figure 14: *Tanδ* Curves during Ageing

Table 4: *Tg* and *Tanδ* Values During Ageing

Time of Ageing	*tanδ*	*Tg* (°C)
Non-Aged	0.99	10.3
15 days	1.34	6.7
30 days	1.35	7.1
60 days	1.28	7.4
120 days	1.37	6.0
270 days	1.08	8.5

The storage modulus (*E'*), shown in Figure 15, compares the results for samples aged up to 270 days. It can be observed an increase in the storage modulus (*E'*) for the first 120 days of ageing. This is probably due to the freezing of the hydraulic fluid within the structure of the material in temperatures below the glass transition. The frozen fluid acts as a mobility arrest of the polymer chains, resulting in an increase of the storage modulus (*E'*). However, after 270 days of ageing, it can be observed a significant decrease in *E'* for all range of temperatures, showing again the loss of rigidity. Assuming that the crosslink density can be estimated by DMA measurements according to the relation of entropic elasticity ($G = \upsilon k_B T$) where υ is the number of crosslinks by volume unit, and k_B is the Boltzmann's constant [27], the decrease of *E'* can be associated to the breaking of the crosslinks caused by the fluid.

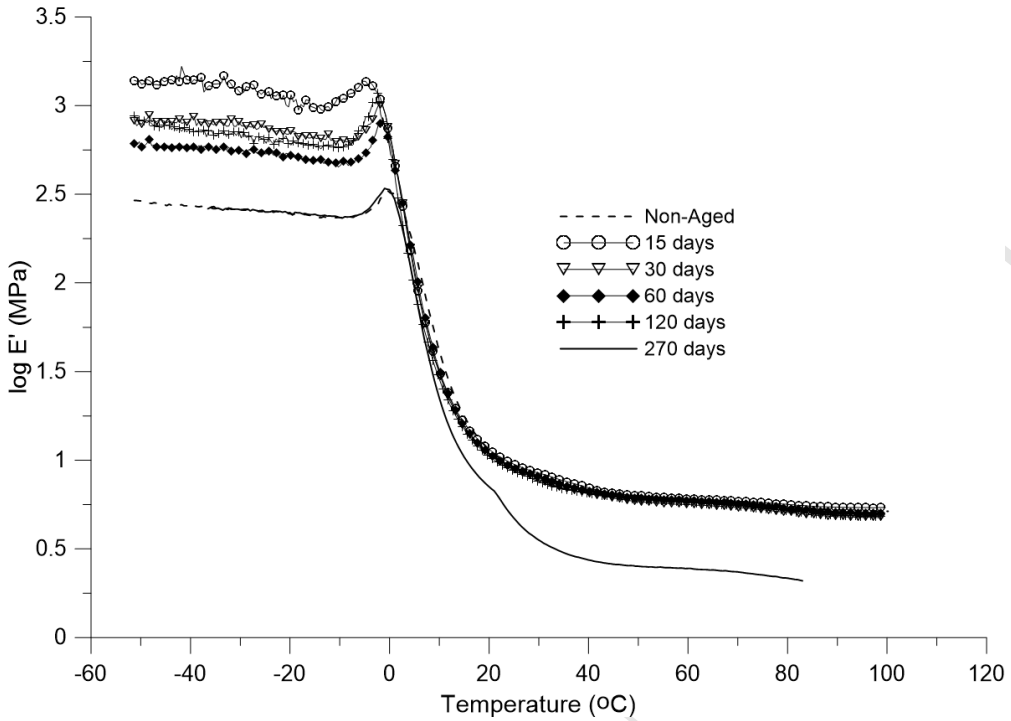

Figure 15: Storage Modulus (E') Curves during Ageing

The results for the uniaxial tensile tests are shown in terms of maximum stress and maximum deformation versus immersion time (Figure 16). It can be noticed an oscillation in stress and strain maximum values during the first 60 days of immersion followed by a stabilization tendency between 120 and 270 days of ageing.

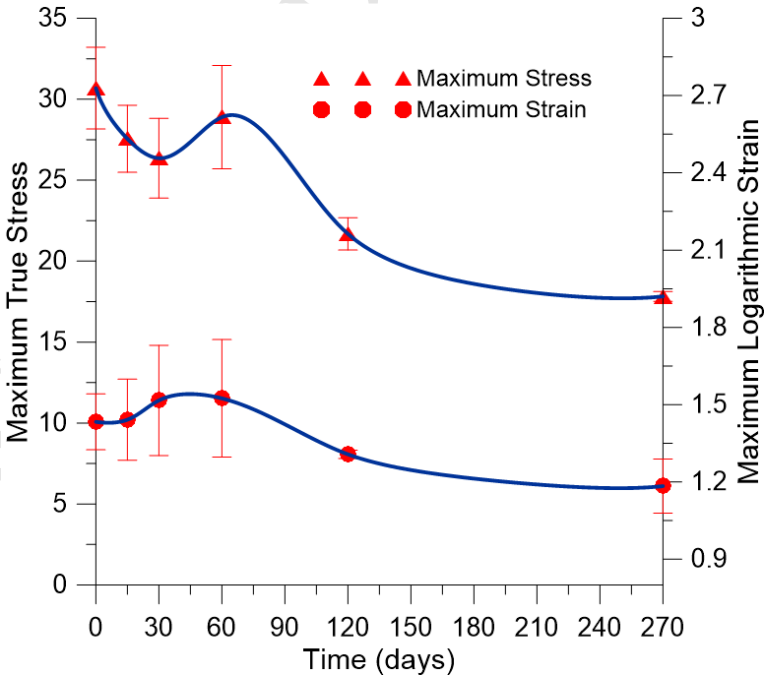

Figure 16: Maximum Stress and Deformation for Aged Samples

To evaluate if ageing have affected the performance of the elastomer for this application, compressive deformation to a tension of 10 MPa (maximum stress value observed in numerical simulations for Viton® liner, Table 2) for the different immersion times are plotted in the graph of Figure 17. It can be noted that the logarithmic compressive deformations stay almost constant (around 40%) during ageing. Moreover, as the major deformations experienced by the hose during operation are compressive ones, the stability of the values observed in Figure 17 indicated that the material can be successfully employed for this application.

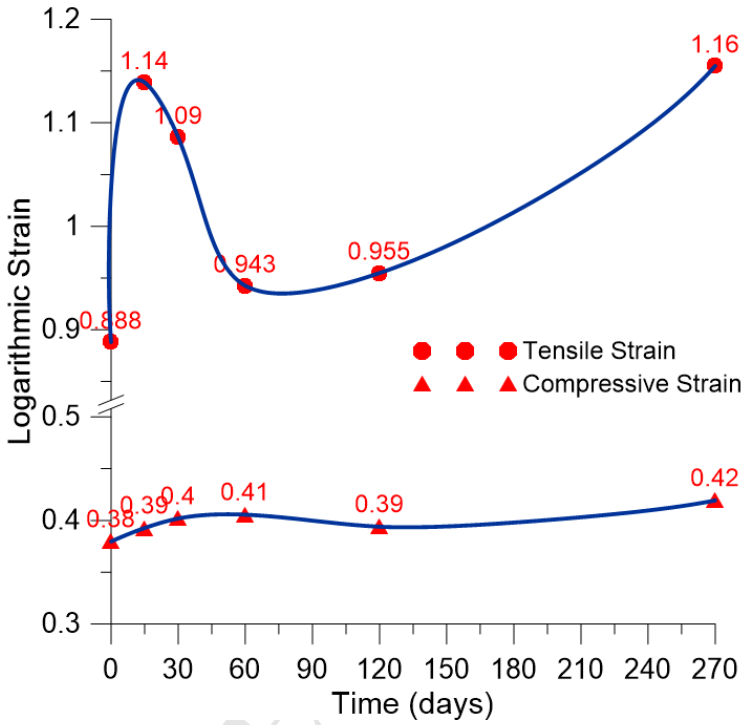

Figure 17: Logarithmic Strain during Ageing for a Fixed Stress of 10 MPa

The changes on the mechanical properties observed for the fluoroelastomer are not an issue of concern within this work. The main changes are observed for times above 120 days considering a constant temperature and steady immersion. Subsea umbilicals are subject to different temperatures along its length. The top end connected to production unit is exposed to sunlight and the subsea end is at 4°C on average. It is also known that the hydraulic fluid is pumped at room temperature to hoses, which only come in contact with the fluid when it is necessary to actuate a xmas tree valve. Thus, the current study is considered conservative whereas exposes the elastomer to hydraulic fluid for 270 uninterrupted days at high temperature (60°C). Moreover, the changes are assigned to break of the crosslink bonds and not to polymer backbone scission, since fluoroelastomers are well known for their excellent temperature resistance up to 200°C [28]. A more suitable crosslink agent can be used to avoid this loss of rigidity and that can operate with each specific hydraulic fluid. One of the great advantages of elastomeric materials is that their properties can be tailored for a specific application. There are various examples that can be found in literature where fluorelastomers in general can have their propertied modified to suit a

specific application [29], [30], [31], [32], [33] and [34]. Furthermore, ageing behavior depends on the type of fluid and it is known that besides water based, methanol or hydrocarbon based fluids can also be transported through umbilical hoses [35]. Therefore, for different fluid compositions, specific ageing studies must be carried to determine if the materials is suitable.

The authors did not find any recommendation practice establishing a criterion to evaluate the performance of aged elastomer for umbilical hoses application. Therefore, the validation of Viton® is based on its performance observed in all mechanical and thermal tests accomplished and further evaluation must be carried out before Viton® or any other fluorelastomer can be recommended for use as hose materials for umbilicals or other similar applications.

Additionally, according to Rabelo [2], due to the loadings suffered by umbilical cables during installation, it is essential to the process to be carried out at completely filled condition. The current study proposes the manufacture of hoses whose elastomeric liner will eliminate such need, since the Viton® does not concentrate deformation, allowing the hoses to remain collapsed during umbilical installation and operation. Such simplification would decrease costs associated to the installation and provide less concern about failure.

5. CONCLUSIONS

This work proposes a new material to manufacture hydraulic hose liners based on the elimination of the failure mode, which may occur during installation, handling and operation of subsea umbilical cables. This study compares the material currently used by industry (PA 11) and a fluorinated elastomer (Viton®) to validate the use of the latter. It should be noted that the evaluation was based on the mechanical behavior of both materials under pressure loads experimented by umbilical cables in service. To this end, material data and samples were collected from manufacturers to enable the accomplishment of mechanical tests and theoretical computer simulations.

Computational simulation results showed that both PA 11 as Viton® liners do not fail after a combined cycle of external (collapse) and internal pressure. PA 11 liner has showed to concentrate very high plastic strains after collapse and even increase it under internal pressure. After a few number of loading cycles, these plastic strains may nucleate a flaw resulting in premature liner failure. The Viton® is a hyperelastic material and does not present plasticity under high total strains (even higher that PA 11 liner), allowing its secure operation under such conditions.

The compatibility between Viton® and the hydraulic fluid driven by the hose was also investigated in this study. All of the mechanical and thermal analysis performed during 270 days of ageing showed that the interaction with the hydraulic fluid causes reduction of rigidity of Viton® due to changes in the degradation mechanism of the material, but without compromise its application. Changes on the crosslinking agent can applied to improve the chemical resistance though.

Therefore, it can be said that Viton® is a good candidate to replace PA 11 to manufacture hydraulic hoses of subsea umbilical cables, provided a qualification program of prototypes can be run by reliable testing laboratories.

6. ACKNOWLEDGMENTS

The authors acknowledge technical and financial support of the ANP Human Resources Program (PRH 35) and CNPq for supporting the research activities and student support for experiments.

7. REFERENCES

1. L. Legallais, M. Stratfold, J. Hardy. A New Generation of Umbilical Hoses. 25th Annual Offshore Technology Conference. Houston, Texas, USA, 3-6 May, 1993.
2. A.S Rabelo. *Representação Numérica de Mangueira Termoplástica de Umbilical Submarino*. Master Thesis, COPPE/UFRJ, Rio de Janeiro, RJ, Brazil, 2013.
3. A. Dobson, I. Probyn et al. Multi-Axis Finite Element Analysis of Helical Umbilical Structures in Bending, Tension and Crushing. Subsea Controls and Data Acquisition 2006: Controlling the Future Subsea. Society of Underwater Technology, 2006.
4. M. Pereira, P.R Ramar, M. Dixon. Installability of Umbilicals. Offshore Technology Conference, Houston, Texas, USA, 5-8 May, 2014.
5. C.P Pesce et al. Structural Behavior of Umbilicals: Part I - Mathematical Modeling. 29th International Conference on Ocean, Offshore and Arctic Engineering. American Society of Mechanical Engineers, 2010.
6. M. Dixon and T. Zhao. 3D Modeling Improves Deepwater Umbilical Design Dependability. Offshore Technology Conference, Houston, Texas, USA, 5-8 May, 2008.
7. V. Le Corre and I.Probyn. Validation of a 3-Dimensional Finite Element Analysis Model of Deep Water Steel Tube Umbilical in Combined Tension and Cyclic Bending. 28th International Conference on Ocean, Offshore and Arctic Engineering. American Society of Mechanical Engineers, 2009.
8. M. Brodesser, W.M Banks et al. The Chemical Compatibility of Thermoplastic Hose Used in Umbilicals. 13th International Offshore and Polar Engineering Conference, Honolulu, Hawaii, USA, May 25-30, 2003.
9. M. Brodesser, W.M Banks and R. A Pethrick. Ageing of Thermoplastic Umbilical Hose Materials Used in a Marine Environment II – Nylon. Journal of Materials Design and Applications. Vol. 228, p. 63-88, 2014.
10. J.D Stables, I.R Dodge and D.A Macraild. More Realistic Method for Predicting the Compatibility of Thermoplastic Hoses When Used in Subsea Umbilical Systems. 25th Annual Offshore Technology Conference. Houston, Texas, USA, 3-6 May, 1993.
11. P.S McCarthy and P.H Knight. The Dynamic Response of Thermoplastic Hoses. Journal Umbilicals the Future, p. 35-64, 1995.
12. ABAQUS, User's and Theory Manuals, Release 6.4, Hibbitt, Karlsson, Sorensen, Inc., 2004.

13. Y.J Xuebao. The Meshless Method for Rubber Hyperelastic Material Based on Yeoh Mode Type Constitutive Laws. Journal of Basic Science and Engineering, 2009.
14. ASTM D638. Standard Test Method for Tensile Properties of Plastics. Annual Book of ASTM Standards. Vol. 08.01, 2014.
15. ASTM D412. Standard Test Methods for Vulcanized Rubber and Thermoplastic Elastomers - Tension. Annual Book of ASTM Standards, Vol. 09.01, 2013.
16. ISO7743. Rubber, vulcanized or thermoplastic- Determination of Compression Stress-Strain Properties. 2008. Third Edition.
17. ASTM 2240-91.Test Method for Rubber Property - Durometer Hardness. 1995. Annual Book of ASTM Standards, vol. 09.01, 1995.
18. ASTM E2254. Standard Test Method for Storage Modulus Calibration of Dynamic Mechanical Analyzers. Annual Book of ASTM Standards, Vol. 14.02, 2013.
19. ASTM D6370. Standard Test Method for Rubber—Compositional Analysis by Thermogravimetry (TGA). Annual Book of ASTM Standards, Vol. 09.01, 2014.
20. X. Chen and S. Hui. Ratcheting behavior of PTFE under cyclic compression. Polymer Testing, vol. 24, n. 7, p. 829-833, 2005.
21. Z. Zhang, X. Chen and T. Wang. A Simple Constitutive Model for Cyclic Compressive Ratchetting Deformation of Polyteterafluoroethylene (PTFE) with Stress Rate Effects. Polymer Engineering & Science, vol. 48, n. 1, p. 29-36, 2008.
22. Z. Zhang and X. Chen. Multiaxial ratcheting behavior of PTFE at room temperature. Polymer Testing, vol. 28, n. 3, p. 288-295, 2009.
23. J. Mohanraj et al. Fracture Behavior of Diedrawn Toughened Polypropylenes. Journal of Applied Polymer Science. Vol. 88, n. 5, p 1336-1345, 2003.
24. D.J.A Senden, G.W.M Peters et al. Anisotropic Yielding of Injection Molded Polyethylene: Experiments and Modeling. Polymer Journal, p. 5899-5908, 2013.
25. I. Banik, A. Bhowmick, S.V Raghavan et al. Thermal Degradation Studies of Electron Beam Cured Terpolymeric Fluocarbon Rubber. Polymer Degradation and Stability Journal, vol. 63, p. 413-421, 1999.
26. J.A Hiltz. Characterization of Fluoroelastomers by Various Analytical Techniques Including Pyrolysis Gas Chromatography Mass Spectrometry. Journal of Analytical and Applied Pyrolysis, vol 109, p. 283-295, 2014.
27. S. Turri et al. Dynamic and Thermo-Mechanical Properties of Some Specialty Fluoroelastomers for Low *Tg* Seal Materials. Journal of Polymer Research, vol. 14, n. 2, p. 141-145, 2007.
28. N.K Sinha, R. Mukhopadhyay and B. Raj. Mechanical Behavior of Fluoroelastomer Considering Long Term Ageing. Nuclear Engineering and Design, vol. 254, p. 89-96, 2013.
29. S.S. Banerjee and A.K. Bhowmick. Tailored Nanostructured Thermoplastic Elastomers from Polypropylene and Fluoroelastomer: Morphology and Functional Properties. Industrial & Engineering Chemistry Research, v. 54, n. 33, p. 8137-8146, 2015.

30. Y. Wang et al. Studies on Self-vulcanizing Fluoroelastomer/Phenol Hydroxy Silicone Rubber Blends. Chinese Journal of Polymer Science, v. 27, n. 03, p. 381-386, 2009.
31. S. Lakshminarayanan, G.A. Gelves and U. Sundararaj. Vulcanization Behavior and Mechanical Properties of Organoclay Fluoroelastomer Nanocomposites. Journal of Applied Polymer Science, v. 124, n. 6, p. 5056-5063, 2012.
32. C. Yamoun and R. Magaraphan. Peroxide Cured Natural Rubber/Fluoroelastomer/High-density Polyethylene via Dynamic Vulcanization. Polymer Engineering & Science, v. 51, n. 8, p. 1484-1488, 2011.
33. J. Wei and J. Qiu. Allyl-Functionalization Enhanced Thermally Stable Graphene/Fluoroelastomer Nanocomposites. Polymer, v. 55, n. 16, p. 3818-3824, 2014.
34. V.V. Chapurkin, V. P. Medvedev and S.V. Chapurkin. Vulcanization of Fluoroelastomers Using Fluorine Peroxides. Russian Journal of Applied Chemistry, v. 88, n. 8, p. 1282-1287, 2015.
35. R.A. Pethrick, W.M. Banks and M. Brodesser. Ageing of Thermoplastic Umbilical Hose Materials Used in a Marine Environment 1 – Polyethylene. Journal of Materials: Design and Applications, v. 228, p. 45-62, 2014.